Int. J. Heat Mass Transfer. Vol. 24, No. 6, pp. 969–982, 1981
Printed in Great Britain

0017-9310/81/060969-14 $02.00/0
Pergamon Press Ltd.

DISPERSION FROM LINE SOURCES IN TURBULENT PIPE FLOW

P. A. DURBIN
Department of Applied Mathematics and Theoretical Physics,
University of Cambridge, Cambridge, U.K.
and
S. FROST
Department of Engineering, University of Cambridge, Cambridge, U.K.

(*Received* 11 *July* 1980 *and in revised form* 10 *September* 1980)

Abstract—Data on the mean and variance of the temperature field downstream of line sources in turbulent pipe flow are presented. We consider both a wall and an elevated source. The existing theory on dispersion is used to describe our measurements of mean temperature; wall source measurements agree well with an eddy diffusion calculation; data obtained with the source elevated agree with the theories of [5] and [7]. The connection of centre-of-mass and relative dispersion with temperature variance is discussed. The ideas generated from this discussion are used to qualitatively describe measured data.

NOMENCLATURE

d,	wire diameter;
h,	source height;
K,	eddy diffusivity;
l,	length of hot wire;
L,	turbulence integral scale;
N,	exponent in mean velocity power law;
IP,	Legendre polynomial;
Pr,	Prandtl number;
r,	radial coordinate;
R,	pipe radius;
Re,	Reynolds number;
S,	source-dependent constant in model of Section 4;
t,	time;
t_η,	Kolmogoroff time-scale;
T, T',	temperature and temperature fluctuation;
T_L, T_θ,	Lagrangian and integral time-scales;
T_f,	flux temperature;
U,	axial mean velocity;
u, v,	turbulent velocities;
x,	axial coordinate;
y, z,	transformed radial coordinates, Section 3;
y,	radial distance from source, Section 4.

Greek symbols

δ,	source size;
$\delta(\cdot)$,	delta function;
η,	Kolmogoroff scale;
κ,	conductivity;
ν,	viscosity;
ω,	frequency;
$\sigma_v, \sigma_x, \sigma_2$,	standard deviation of velocity and of particle trajectories;
τ,	correlation delay time.

Superscripts

$\tilde{\ }$,	dimensional quantities;
$\bar{\ }$,	average quantities.

1. INTRODUCTION

THIS study was undertaken to provide data on the mean and variance of temperature fluctuations produced by a line source in a simple turbulent flow. We have chosen to study dispersion in pipe flow because it is a well-defined equilibrium flow, devoid of entrainment interfaces which complicate free turbulent shear flows, which has considerable practical application. A line source was chosen because it is the simplest to construct and is the source to which one's curiosity is first directed.

A knowledge of the variance of a dispersing contaminant is becoming increasingly important in applications of turbulent dispersion; such as in air pollution, combustion and nuclear safety studies. However, experimental data on $\overline{T'^2}$ is notably lacking in the literature. Perhaps this is because of the lack of a ound theoretical framework within which to interpret uch data. Here we will discuss the origin of the intractability of the fluctuation problem for line sources, and present some ideas which may shed light on it.

On the contrary, a very reasonable theoretical base exists for the problem of mean dispersion. It will be used to describe our experimental findings.

2. APPARATUS AND FLOW MEASUREMENTS

Apparatus

Our experiments were performed in a 20 cm dia. open circuit copper pipe. An upstream development length of 25 pipe diameters was allowed, with a test section of 15 diameters (Fig. 1). Nichrome wire (d

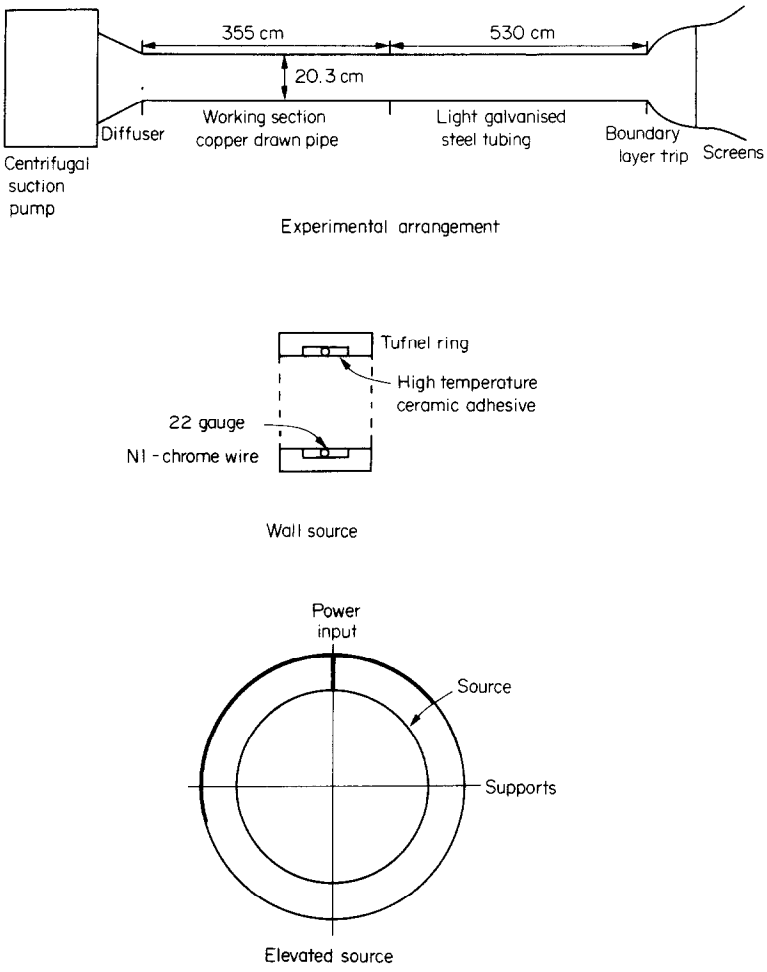

FIG. 1. Diagram of experimental rig and source configurations.

= 2 mm) was used as the temperature source. Both wall and elevated sources were used.

The wall source was constructed by embedding the NiCr wire in the inside of an insulating Tufnel ring, which was then fitted into a groove in the side of the pipe. The elevated source was constructed by suspending a circular loop of wire on an X-frame of 3 mm dia steel rods. The wire was insulated from the rods and all temperature measurements were made in the mid-plane of the X. The electrical heating of the wire was controlled with a Variac transformer. Measurements were made with various wire heating rates. Thereby we verified that our normalised results were independent of heating rate.

With the elevated source in position, the RMS axial velocity was measured at one pipe diameter downstream of the source and compared to the undisturbed case. No significant disturbance to the turbulence was found.

Mean velocities were measured both by a pitot-tube and by a single hot wire. Velocity fluctuations were measured with DISA type 55M constant temperature anemometers ($d = 5\,\mu$m, $l/d = 200$). The signal from the anemometers was passed through DISA type 55D30 linearisers, high pass and low pass filtered at 0.5 Hz and 2.5 kHz, then recorded on magnetic tape for analysis. Temperature measurements were made with DISA type 55M constant current anemometers ($d = 1\,\mu$m, $l/d = 400$). The current in the wire was kept sufficiently small to ensure that temperature measurements were not contaminated by velocity fluctuations. This was achieved by measuring the temperature in the unheated pipe, for various velocities, reducing the current until there was no velocity dependence. The frequency response of the probes was found to be just over 2 kHz, well above the Kolmogoroff frequency in the experiments. The temperature signals were analysed in the same way as the velocity signals, with the obvious exception of the linearisers. Calibration of probes took place at the start and end of each run, to check for the possibility of drift in the electronics. Means, variances and correlations were computed from 1.2×10^5 data points. Larger amounts of data did not change the values.

Before each run it was checked that the flow was fully developed by verifying the linearity of the Rey-

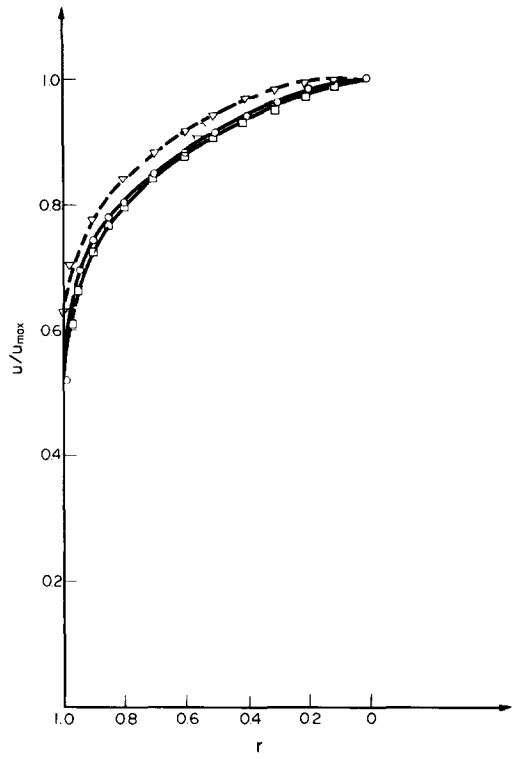

FIG. 2. Mean velocity profile, $Re = 2.5 \times 10^5$ —○—, —□—, 1/7th power law, Laufer ($Re = 5 \times 10^5$), ---▽---.

Table 1. Turbulence scales

U (m/s)	u_* — skin friction velocity $Re = U_{max} D/\nu$	u_* (m/s)
4.0	5.0×10^4	0.18
9.9	1.2×10^5	0.56
20.0	2.5×10^5	1.04

Stream integral length scales of radial and axial velocities ($Re = 2.5 \times 10^5$)

			(Sabot and Comte-Bellot)	
r	L_u/R	L_v/R	L_u/R	L_v/R
0.9	1.00	0.06	0.98	0.06
0.5	1.03	0.09	1.01	0.12
0.0	0.92	0.12	0.62	0.13

Microscale ($Re = 2.5 \times 10^5$)

r	λ (mm)
0.0	3.62
0.125	3.31
0.25	3.59
0.5	3.80

nolds stress and the constancy of the fluctuating velocity at stations 1, 2, 4, 8 and 15 diameters along the test section.

The overall accuracy of mean measurements, based on the limitations of the hot-wire equipment and on repeatability of measurements, was 5%, whereas that of the RMS was 10%.

Flow measurements

Figure 2 shows the mean velocity distribution and its seventh power law fit, compared with [1]. The difference between the pair of measurements is accounted for by difference in Reynolds number. The three velocity fluctuation intensities and Reynolds stress are shown in Fig. 3. These data agree favourably with those of [1], but the u (axial) and v (radial) components show some discrepancy when compared with Sabot and Comte-Bellot's [2] data. Because of its relevance to dispersion, we include, in Fig. 4, a spectrum of v'. Table 1 lists values of friction velocity, integral scales and microscales. Values of L_v are in agreement with Sabot and Comte-Bellot, while L_u shows a discrepancy at the centre of the pipe.

3. WALL SOURCE

Diffusion analysis

The criterion for validity of the eddy diffusion model for mean dispersion is that one considers processes on a time-scale large compared to the Lagrangian time-scale (T_L). Since $T_L \to 0$ near the pipe wall we expect eddy diffusion to apply at all times to dispersion from the wall source. Hence we consider the equation

$$\tilde{U}(\tilde{r})\frac{\partial \tilde{T}}{\partial \tilde{x}} = \frac{1}{\tilde{r}}\frac{\partial}{\partial \tilde{r}}\left(\tilde{r}\tilde{K}(\tilde{r})\frac{\partial \tilde{T}}{\partial \tilde{r}}\right) \quad (1)$$

where $\tilde{}$ indicates the variables are dimensional. Our mean velocity is matched reasonably by a power law,

$$\tilde{U} = \bar{U}[1 - (\tilde{r}/R)^2]^{1/N}(N+1)/N,$$

with $N = 7$, see Fig. 2. $\bar{U}$ is the radial average mean velocity. An eddy diffusivity suitable in the present case is

$$\tilde{K} = 9.2/Pru_*R[1 - (\tilde{r}/R)^2].$$

This is the simplest form which satisfies the constraints $d\tilde{K}/d\tilde{r} = 0$ at $\tilde{r} = 0$,

$$\tilde{K} = 0.2/Pru_*R[1 - (\tilde{r}/R)^2].$$

as $\tilde{r} \to R$: the first constraint follows from symmetry, the second from surface layer theory, with von Karman's constant equal to 0.4 and Pr the turbulent Prandtl number. The parabolic form for $\tilde{K}$ has been found appropriate in several similar studies of turbulent dispersion (see [3] Fig. 2). The flux temperature

$$T_f \equiv 2\int_0^R \tilde{U}(\tilde{r})\tilde{T}(\tilde{r})\tilde{r}d\tilde{r}/\bar{U}R^2$$

is a constant, according to (1), and it, along with R, $\bar{U}$

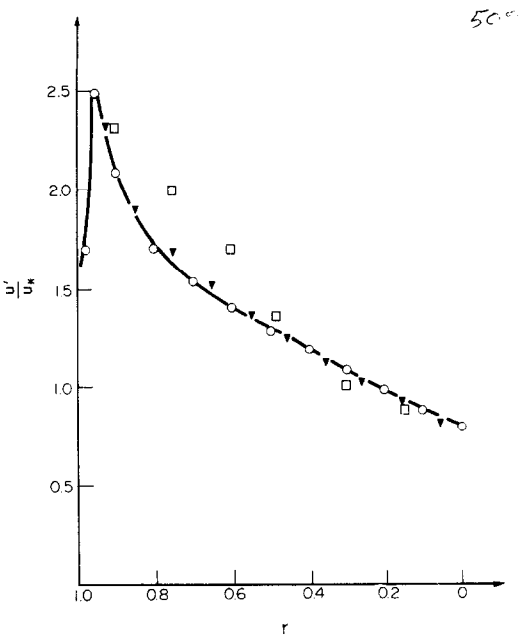

FIG. 3(a).

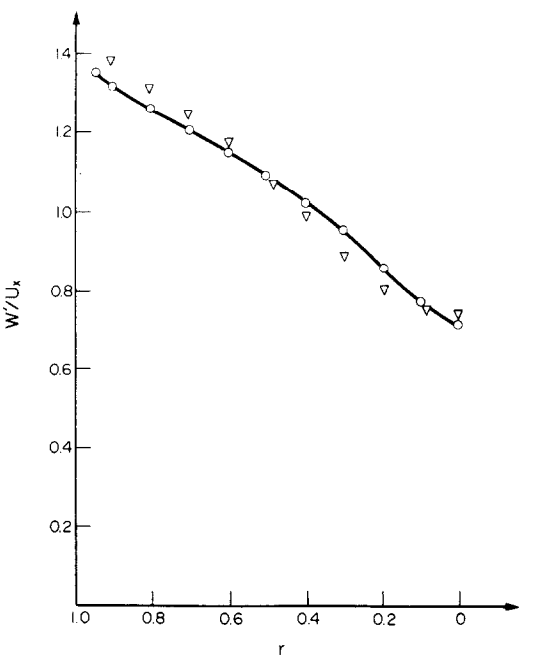

FIG. 3(b).

and u_* are used to non-dimensionalise variables:

$$r = \tilde{r}/R, \quad x = \tilde{x}u_*/R\bar{U},$$
$$T = \tilde{T}/T_f, \quad K = \tilde{K}/u_*R, \quad U = \tilde{U}/\bar{U}.$$

This non-dimensionalisation of x eliminates Reynolds number dependence and was found to collapse our experimental data. We also introduce the new independent variable $y = 1 - 2r^2$, so that (1) transforms to

$$U\frac{\partial T}{\partial x} = \frac{0.8}{Pr}\frac{\partial}{\partial y}(1-y^2)\frac{\partial T}{\partial y}. \tag{2}$$

Here $-1 \leq y \leq 1$. The solution to (2) satisfies

$$\tfrac{1}{2}\int_1^1 UT\mathrm{d}y = 1,$$

and initially $T = 0$ if $y \neq -1$. In order to find a solution satisfying these constraints we introduce a further coordinate change,

$$\frac{z+1}{2} = \frac{1}{2}\int_{-1}^{y} U(y)\mathrm{d}y = \left(\frac{y+1}{2}\right)^{1+N/N}. \tag{3}$$

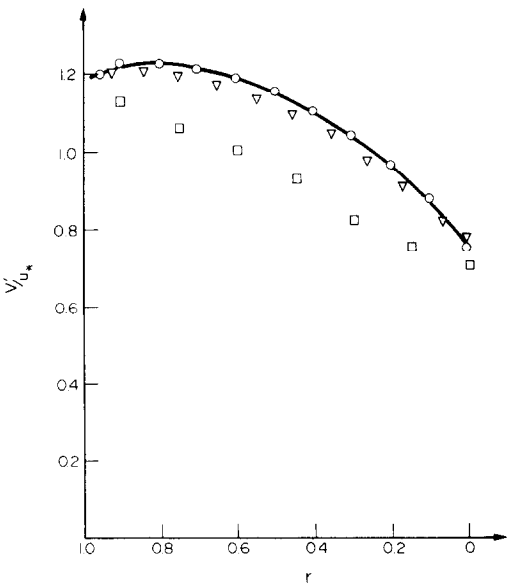

FIG. 3(c).

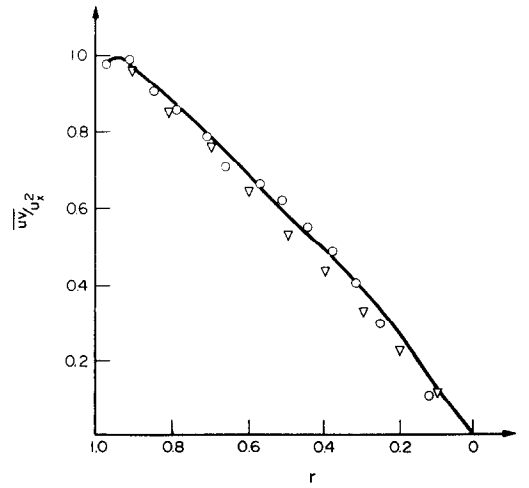

FIG 3.(d).

FIG. 3. Turbulent velocity measurements, $Re = 2.5 \times 10^5$. —○—, Laufer, △; Sabot and Comte-Bellot, □. (a) Axial fluctuation profile. (b) Radial fluctuation profile. (c) Tangential fluctuation profile. (d) Reynolds stress profile.

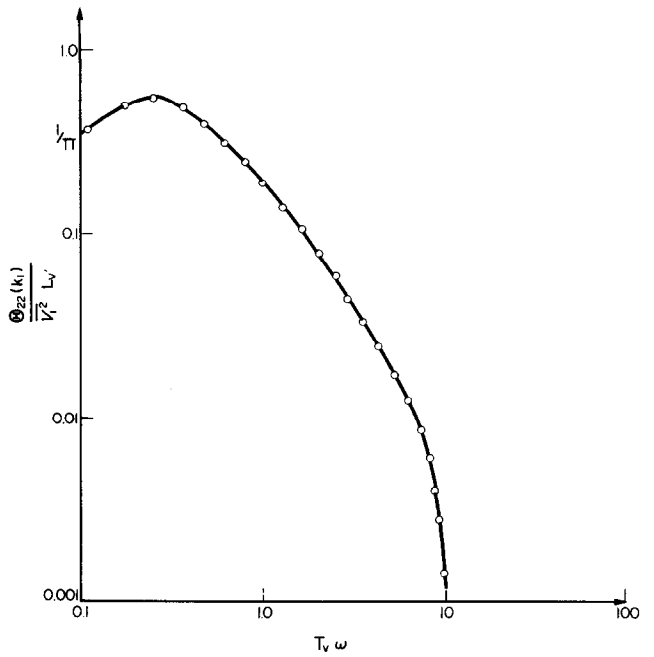

FIG. 4. Spectrum of radial velocity fluctuations at $r = 0.0$.

After the transformation (3), equation (2) assumes a complicated form, but in the limit of large N it is adequately approximated by

$$\frac{\partial T}{\partial x} = \frac{0.8}{Pr}\frac{\partial}{\partial z}(1 - z^2)\frac{\partial T}{\partial z} \tag{4}$$

and the initial condition is now simply

$$T = 2\delta(z + 1), \quad x = 0. \tag{4'}$$

The large N approximation is really an assumption that the mean velocity shear is only significant in a thin layer near the wall. Now that N has served its purpose as an ordering parameter in the derivation of (4), we will set it equal to 7.

A solution to (4) and (4') is

$$T = \sum_{n=0}^{\infty} (2n + 1)(-)^n \mathbf{IP}_n(z)\exp(-0.8n(n + 1)x/Pr) \tag{5}$$

where $\mathbf{IP}_n$ is a Legendre polynomial. In additional (5) we will want to know the first and second plume moments,

$$\bar{r^n} = 2\int_0^1 U(r)T(r)r^{n+1}\,dr = \frac{1}{2}\int_{-1}^{1} T(z)r^n(z)dz, \tag{6}$$

$n = 1, 2$. Using (5),

$$r(z) = [1 - [(z + 1)/2]^{7/8}]^{1/2}$$

and the Rodrigues formula for $\mathbf{IP}_n$, we find

$$\left.\begin{aligned}\bar{r} = \frac{4\sqrt{\pi}}{7}\sum_{n=0}^{\infty}\sum_{m=0}^{\infty}\frac{(2n + 1)(-)^m(n + m)!}{m!m!(n - m)!} \\ \times\frac{\Gamma\left(\frac{8m + 8}{7}\right)}{\Gamma\left(\frac{16m + 37}{14}\right)}\exp\left(\frac{-0.8}{Pr}n(n + 1)x\right)\end{aligned}\right\} \tag{7}$$

$$\left.\begin{aligned}\bar{r^2} = 1 - \frac{8}{15}\Gamma^2(15/8)\sum_{n=0}^{\infty}\frac{(2n + 1)}{\Gamma\left(\frac{15}{8} - n\right)} \\ \times\Gamma\left(\frac{15}{8} + n\right)\exp\left(\frac{-0.8}{Pr}n(n + 1)x\right).\end{aligned}\right\}$$

The value $Pr = 0.8$ was found appropriate to our experimental data. All theoretical results will be presented for this value. A turbulent Prandtl number of 0.8 is well within accepted values. Indeed Robbins and Fackerell [4] found $Pr = 0.6$–0.7 was required to fit their data on boundary layer dispersion.

Measurements, compared with diffusion analysis

Measured mean temperatures at various downstream locations are shown in Fig. 5 by solid lines with crosses and are compared with the solution (5), shown by dashed lines. The experimental profiles are non-dimensionalised by the value of T_f corresponding to that profile. This is because a small amount of heat

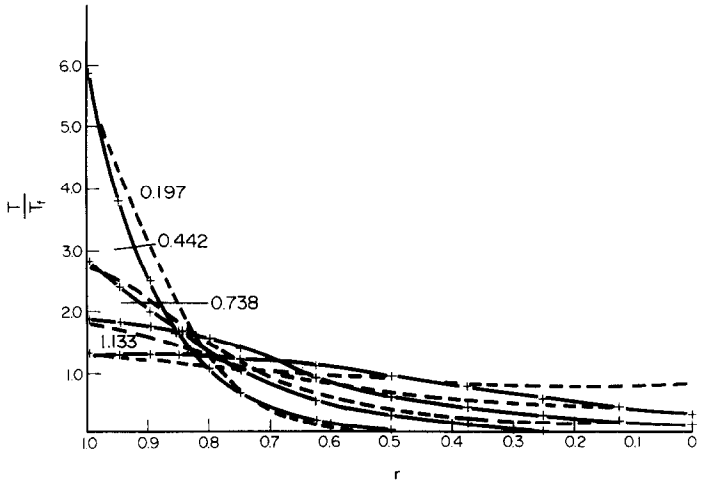

FIG. 5. Measured profiles of mean temperature, $Re = 5 \times 10^4$. Numbers indicate x-position, + —— + data, – – – diffusion calculation.

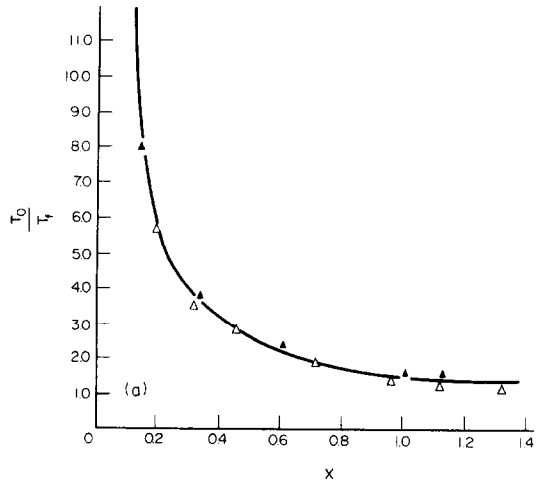

FIG. 6(a). Wall temperature vs x. △, $Re = 5 \times 10^4$; ▲. $Re = 1.2 \times 10^5$; ——, theory.

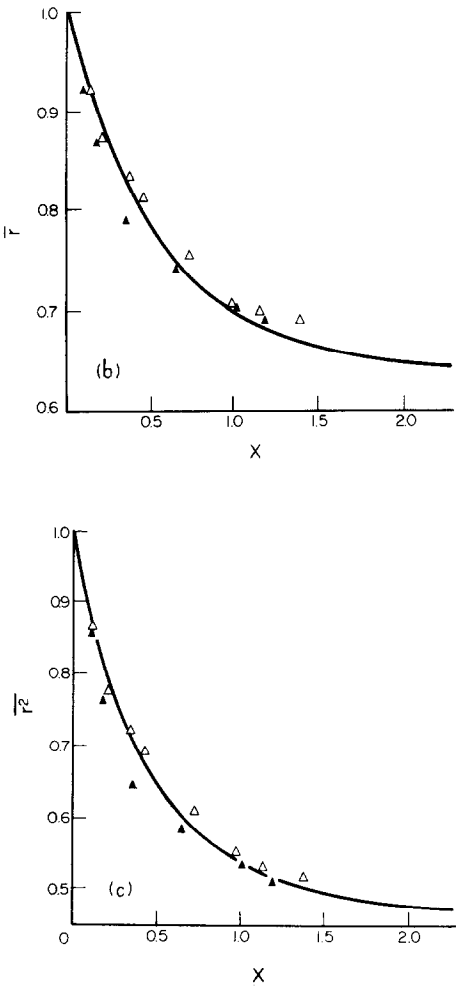

FIG. 6(b, c). First and second plume moments, as defined by equation (6). Symbols as in Fig. 6(a).

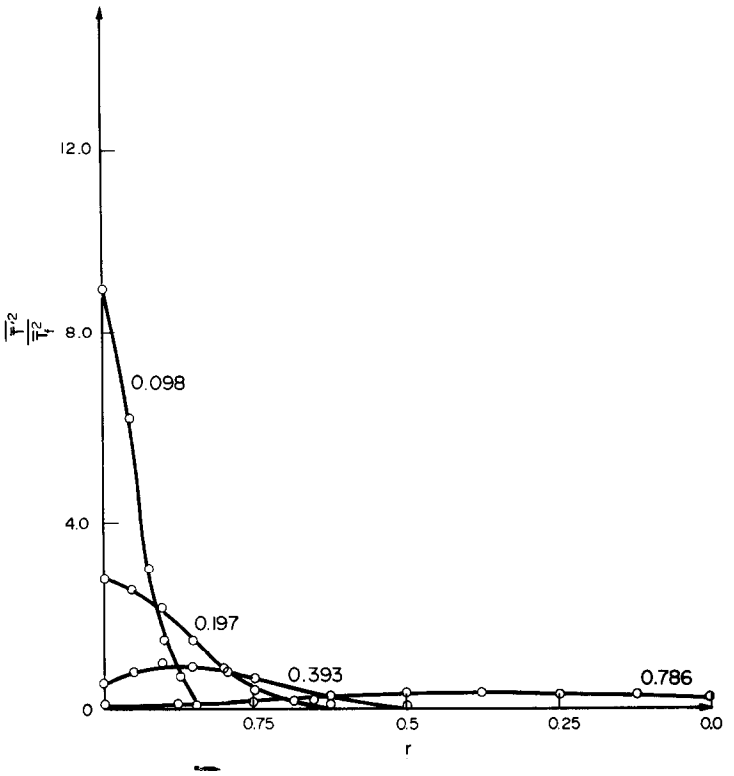

FIG. 7. Profiles of $\overline{T'^2}$ at distances downstream of wall source, $Re = 5 \times 10^4$.

was conducted along the pipe wall and it was only after 2 pipe diameters ($x \approx 0.17$) that T_f became constant.

Allowing for experimental uncertainty and, in the measurements at $x = 0.197$, for the rapid initial change of the profile with x, the agreement between experiment and theory is quite good. The major discrepancy is that the diffusion calculation has heat reaching the centre of the pipe more rapidly than observed.

Further comparison between our diffusion analysis and data is given in Figs. 6(a)–(c), where we have plotted wall temperature and first and second plume moments: symbols are data and solid lines are theory. The agreement in all cases is quite good and it can be seen that our non-dimensionalisation of x does indeed collapse measurements made at $Re = 1.2 \times 10^5$ and at $Re = 5.0 \times 10^4$. Of course, dimensional values for x can be determined from the information supplied in Table 1, but the reader might find it helpful if we note that the x-units in Fig. 6 are approximately twenty pipe radii.

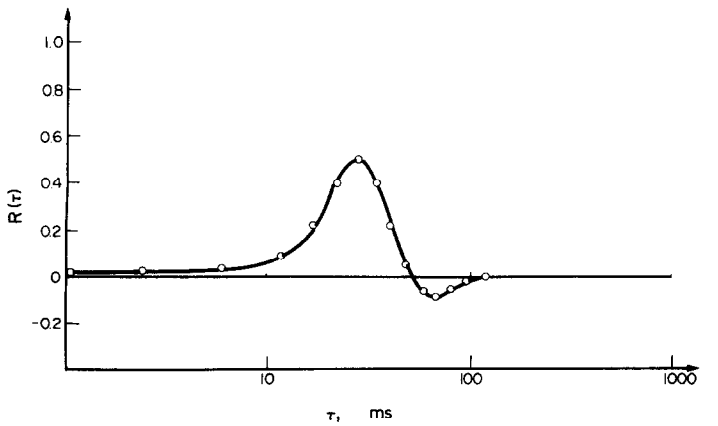

FIG. 8. Correlation between temperatures at $x = 0.08$; $r = 0.95$ and $x = 0.16$; $r = 0.95$ vs time delay. $Re = 5 \times 10^4$.

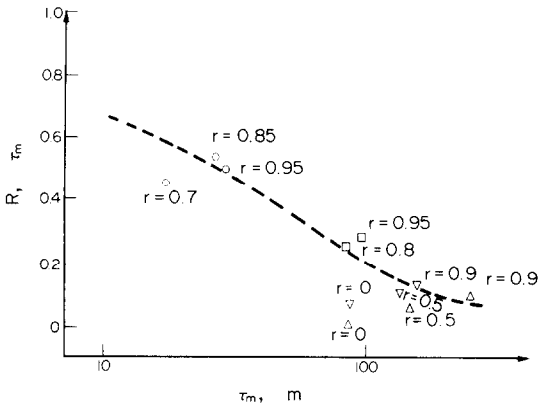

FIG. 9. Value of peak correlation between temperature at $x = 0.08$, $r = 0.95$ and various downstream locations, plotted against the time-delay at which the peak occurred. ○, $x = 0.085$; □, $x = 0.254$; ▽, $x = 0.425$; △, $x = 0.765$; $Re = 1.2 \times 10^5$. – – – trend.

Temperature variance

We present a set of measurements of temperature variance in Fig. 7. These measurements are for $Re = 5.0 \times 10^4$, but the profiles at $Re = 1.2 \times 10^5$ show similar behaviour, except near the wall. At the higher Reynolds number, fluctuations drop suddenly at the lowest measurement point (1.9 mm from the wall). It is possible that this is due to the greater presence of small-scale structure adjacent to the wall at higher Re.

Time-delayed temperature cross-correlations were measured with one probe fixed at $x = 0.08$, $r = 0.95$ and the other probe free to move in both axial and radial directions. Records were made of the cross-correlation as a function of time-delay: Fig. 8 shows a typical curve. Here the second probe is at $x = 0.16$, $r = 0.95$. The peaks of the correlation curves occurred at a time delay which, when multiplied by the local mean velocity, gave a distance equal to the streamwise probe separation. This suggests that axial transport of the variance is due mainly to mean convection.

The data obtained from other measurements, of the type illustrated by Fig. 8 are summarised in Fig. 9. This figure presents a plot of the peak value of the correlation against its time delay, for various probe positions. It can be seen that significant correlations persist up to a streamwise separation of 9 pipe diameters. The dashed line in Fig. 9 is to guide the eye along the gradual decrease in correlation with τ.

In the region near the wall, the integral scale of the turbulence is small. Small scale turbulence can smooth out temperature fluctuations. Consequently, $\overline{T'^2}$ decays quite rapidly with downstream distance (Fig. 7). Because the turbulence near the wall is of smaller scale than in the centre of the pipe, the ratio of fluctuation to mean downstream of a wall source will be low compared to that downstream of an elevated source. For this reason, and because of the great difficulty of understanding the effects of inhomogeneity and mean shear on $\overline{T'^2}$, we decided to shift our study of

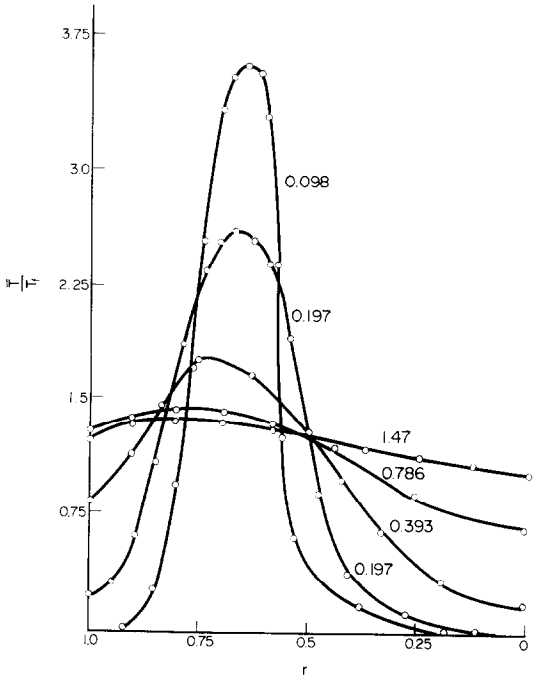

FIG. 10. Mean temperature profiles downstream of elevated source, $Re = 5 \times 10^4$.

fluctuations to a more central region of the pipe where turbulence scales were larger and almost homogeneous. Therefore, the elevated source shown in Fig. 1 was constructed, with the heated wire at $r = 0.675$.

4. MEASUREMENTS WITH SOURCE ELEVATED

Mean temperatures

For an elevated source we expect the dispersion to initially resemble that in homogeneous turbulence. Hence, the mean profiles will be Gaussian. Their variance will increase as $v'^2 t^2$ for $t \ll T_L$ and will be less than this when $t \gtrsim T_L$ [5].

In Fig. 10 we show our measurements of T, and they appear Gaussian for $x \lesssim 0.2$. Our first measurement, at $x = 0.049$, is not included because it would go off scale. Measurements at $Re = 1.2 \times 10^5$ were similar to those in Fig. 10. We estimate the standard deviation (σ_x) of our profiles at $x = 0.042$, 0.049, 0.085, 0.098, 0.169 and 0.197 to be $\sigma_x = 0.03$. 0.04, 0.07, 0.08, 0.11 and 0.13. We would expect $\sigma_x \approx v'\tilde{x}/\tilde{U} \sim x$ for the first few measurements, and this seems to be borne out by observation.

The last few profiles in Fig. 10 show the peak mean concentration descending slightly towards the wall, before the profile becomes flat. The peak descends because the turbulent diffusivity decreases towards the wall.

The qualitative behaviour we found for the temperature profile — Gaussianity, followed by the peak descending towards the wall and, finally, by well-mixedness — was also found by Shlien and Corrsin [6] in their experiments on mean dispersion from line

sources in a boundary layer. An analysis of Shlien and Corrsin's experiments is given by Durbin and Hunt [7]. Durbin and Hunt describe dispersion from elevated sources in terms of: a near field, quasi-homogeneous, region — where the plume is Gaussian; a far-field region, where inhomogeneity plays an essential role, but where the diffusion approximation is applicable; and a transition region, matching the near field to the far field. This description also applies to the present experiments.

The difficulty of describing $\overline{T'^2}$ *theoretically*

At present, methods for predicting $\overline{T'^2}$ are in a stage of early development and are beset by uncertainties [8]. This is, undoubtedly, a reflection of the complexity of the phenomenon being dealt with. In the following some new ideas about the physics of production and destruction of temperature variance are presented. Of course, these physics could be described in terms of production, convection, diffusion and dissipation of $\overline{T'^2}$ (see [8]). But, in the present case, the balance between these processes is quite intricate — in particular, the often made assumption that production and dissipation balance is not valid. The concepts described below enable an equally useful, alternative understanding of concentration fluctuations. We hope that, in conjunction with existing ideas, they will contribute to resolving some uncertainties of the $\overline{T'^2}$ problem.

We will introduce the fluctuation problem by considering an extremely unrealistic model, which describes the infinitesimal-time behaviour of dispersion from an ideal point source. The intuition gained from this consideration will be used to extrapolate to more realistic situations.

Consider heated fluid parcels released into homogeneous turbulent flow and times so short that gradients of turbulent velocity can be ignored; in other words, consider times small compared to the Kolmogoroff time-scale (t_η). It follows that the temperature of these parcels satisfies

$$\frac{\partial T}{\partial t} + \mathbf{u} \cdot \nabla T = k \nabla^2 T \tag{8}$$

where $\mathbf{u}$ is the turbulent velocity and k the molecular diffusivity. Let the source of heated parcels be the plane $y = 0$; so we are considering dispersion in one dimension and time, in analogy to the experimental situation. The solution to (8) with this source is

$$T = \frac{F}{(4\pi k t)^{1/2}} \exp[-(y - Vt)^2/4kt] \tag{9}$$

where F is a constant. Assuming v to be a Gaussian random variable with mean zero and variance σ_v^2, and averaging T and T^2 over all values of v, gives

$$\bar{T} = \frac{F}{(2\pi(\sigma_x^2 + 2kt))^{1/2}} \exp[-y^2/2(\sigma_x^2 + 2kt)] \tag{10}$$

$$\overline{T'^2} = \frac{F^2}{4\pi(kt(\sigma_x^2 + kt))^{1/2}} \times \exp[-y^2/2(\sigma_x^2 + kt)]. \tag{10'}$$

We have written $\sigma_x^2 = \sigma_v^2 t^2$. Although derived for $t < t_\eta$, (10) will clearly describe $\bar{T}$ for longer times; provided σ_x^2 is the variance of the position of dispersing particles (and the turbulent Péclét number is large).

Such is not the case for equation (10'). (10) and (10') give

$$\frac{\overline{T'^2}(y=0)}{\bar{T}^2(y=0)} = \frac{\sigma_x^2 + 2kt}{2((\sigma_x^2 + 2kt)kt)^{1/2}} - 1. \tag{11}$$

If $\sigma_x^2 \gg kt$ this implies, incorrectly, that $\overline{T'^2} \gg \bar{T}^2$. The error is easy to trace.

The spreading of the $\bar{T}$ profile is determined primarily by the randomness of vt in (9); or, more generally, by randomness of the centre-of-mass of instantaneous profiles of $\bar{T}$. Hence (10), which accounts for this randomness, is a good description of $\bar{T}$. Unlike $\bar{T}$, $\overline{T'^2}$ is not a conserved quantity and it depends on more than spreading by centre-of-mass dispersion. Small scale turbulent eddies [the velocity gradients ignored by (9)] can smooth instantaneous profiles of T. It is because these profiles are squared before computing $\overline{T'^2}$ that the role of small-scale turbulent processes in destroying $\overline{T^2}$ cannot be ignored.

Unfortunately, (9) permits only molecular diffusion to smooth instantaneous temperature profiles, while, in practice, turbulent relative dispersion will be the dominant process for smoothing profiles [9]. (The fact that the final step in smoothing fluctuations involves molecular diffusion is irrelevant at high Péclét number, because it is rate-limited by relative dispersion.) Clearly, $\overline{T'^2}$ is quite sensitive to small scales of turbulent motion. $\bar{T}$ is insensitive to them, depending mainly on the bodily dispersion of individual heated parcels and not on the relative motion of pairs of parcels.

In (10') $\sigma_x^2 + kt$ is the mean-square dispersion of the centre-of-mass of a pair of parcels in relative motion due to molecular diffusion. This suggests we might, more generally, replace $\sigma_x^2 + kt$ by σ_2^2, the centre-of-mass dispersion of two parcels in relative motion due to turbulent dispersion. This incorporates the effect of turbulent relative dispersion on the spatial structure of $\overline{T^2}$. Its, more important, effect on the amplitude of $\overline{T^2}$ is not as easy to deduce. Compounding this difficulty is the limitation of (10') to an infinitesimal source. In practice our source was large compared to the Kolmogoroff scale, η, and this also effects the amplitude of $\overline{T^2}$ in (10').

It is the factor of $(kt)^{-1/2}$ in (10') which must be replaced by a representation of the effect of relative dispersion: as it stands, this term represents decay of $\overline{T^2}$ by molecular diffusion unaided by small-scale turbulence. Durbin [9] presented a stochastic model to represent relative dispersion. We describe his results below.

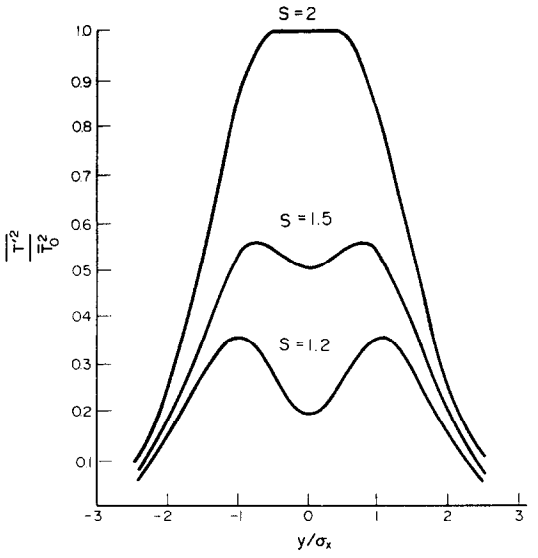

FIG. 11. $\overline{T'^2}$ profiles as given by equation (13).

The model described in [9] relates relative dispersion and contaminant fluctuations for distributed sources. A line source is treated there as the asymptotic limit of a small distributed source, assuming the source to remain large compared to η, while becoming small compared to the integral scale, L. After asymptotic analysis the expression

$$\frac{\overline{T^2}}{F^2} = \frac{S}{2\pi\sigma_x\sigma_2}\exp(-y^2/2\sigma_2^2) \tag{12}$$

was obtained. Here S is a constant which depends on the source size. The factor S/σ_x arises from the relative dispersion model used by Durbin. It represents the reduction of $\overline{T^2}$ which occurs when fluid parcels with differing concentrations are mixed together by turbulent relative dispersion. S increases, slowly, as the ratio, L/δ, of integral scale to effective source size increases. (Actually, Durbin had σ_x in place of σ_2 but his model suggests the modification (12).) σ_2 depends on the instantaneous average velocity of a particle pair $[(v_1 + v_2)/2]$ and so, generally, will be less than σ_x; $\frac{1}{2}\sigma_x^2 < \sigma_2^2 \leq \sigma_x^2$.

From (12) and (10) we obtain

$$\frac{\overline{T'^2}}{\bar{T}^2(y=0)} = \frac{S\sigma_x}{\sigma_2}\exp(-y^2/2\sigma_2^2) - \exp(-y^2/\sigma_x^2) \tag{13}$$

When $(t/T_L)^3 \ll 1$, and the source size is $\ll L$, we may let $\sigma_2^2 \approx \sigma_x^2$ and obtain the $\overline{T'^2}$ profiles depicted in Fig. 11.

Because of the simplicity of the model used to derive it, Fig. 11 should be considered only qualitative. This figure suggests that when the effective source size is large enough (S small enough) $\overline{T'^2}$ will develop a double peaked form. The double peak appears then because dissipation is able to reduce $\overline{T^2}$ sufficiently. The appearance of the double peak also depends on the fact that $\bar{T}^2$ has a narrower profile than $\overline{T^2}$, so that $\bar{T}^2$ is comparable to $\overline{T^2}$ in a central region of the plume but much smaller elsewhere, equation (13).

Measurements of temperature variance

Figures 12(a) and (b) show our measurements of $\overline{T'^2}$, non-dimensionalised by T_f^2. The ratio of fluctuation to mean temperature is higher than for the wall source, although again fluctuations decay very rapidly downstream. The $\overline{T'^2}$ profiles show a double peak. As we have explained, the appearance of the double peak in $\overline{T'^2}$ is simply an indication of the importance of small-scale mixing. Were relative dispersion less effective at reducing $\overline{T^2}$ the peak would not be double.

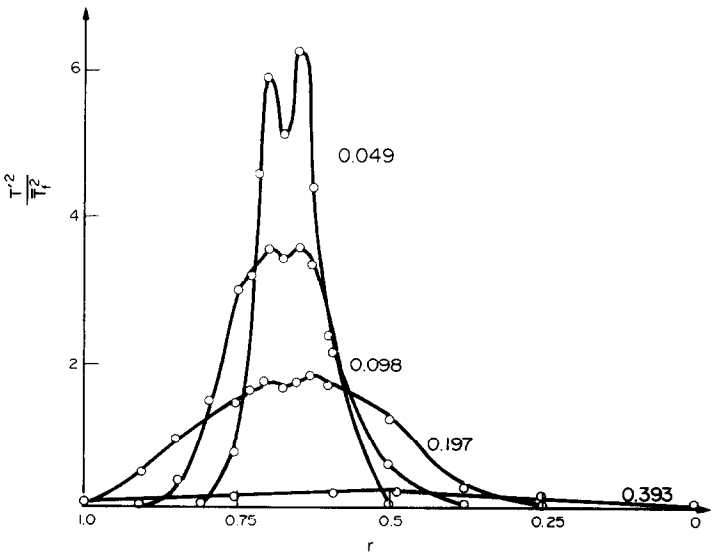

FIG. 12(a).

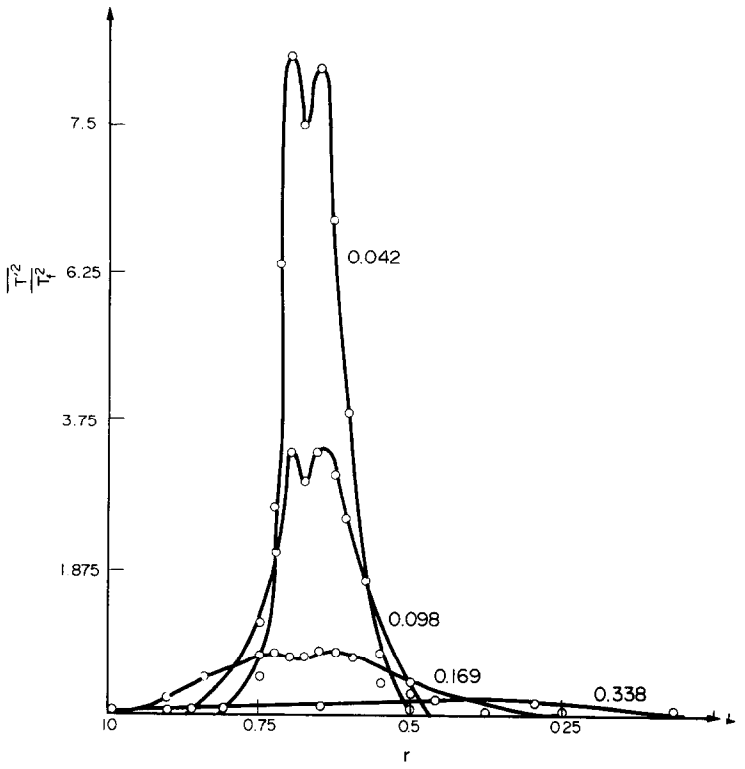

FIG. 12(b).

FIG. 12. Measured $\overline{T'^2}$ profiles downstream of elevated source. Numbers indicate x-position. (a) $Re = 5 \times 10^4$; (b) $Re = 1.2 \times 10^5$.

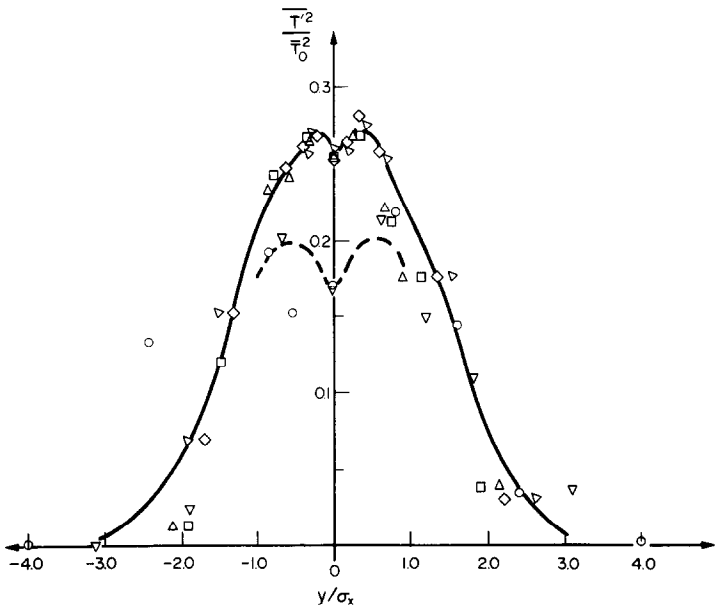

FIG. 13. Data of Fig. 12 replotted as $\overline{T'^2}/\bar{T}^2_{max}$ vs y/σ_x. ○, $x = 0.042$; ▽, $x = 0.049$; □, $x = 0.085$; △, $x = 0.098$; ▷, $x = 0.169$; ◇, $x = 0.197$.

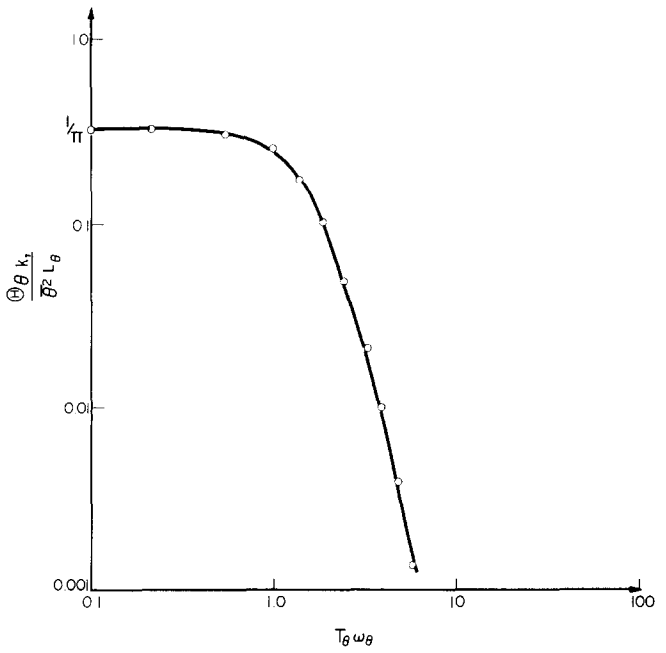

FIG. 14. Spectrum of temperature fluctuations at $r = 0.0$, scaled on T_θ.

Although we found no significant alteration of turbulent intensity, at one pipe diameter downstream, by the source wire, it is inevitable that a small-scale turbulent wake existed behind the wire. This wake would make the effective source size larger than the heated wire's diameter. The small-scale mixing by wake turbulence would also lead to reduction of $\overline{T^2}$, while having little effect on $\bar{T}$. Perhaps this contributed to the appearance of the double peak.

In Fig. 13 we investigate the similarity structure of the $\overline{T'^2}$ profiles. We have plotted

$$\overline{T'^2}(r - h/\sigma_x)/\bar{T}^2(r = h),$$

h being the source height. The profiles have similar spatial structure when plotted in this way, but the amplitudes of the first profiles (at $x = 0.07$ and 0.08) are less than those further downstream. Our explanation is, again, that small scale turbulence in the wake of the source reduces $\overline{T^2}$, relative to $\bar{T}^2$, more effectively than does the larger-scale pipe turbulence.

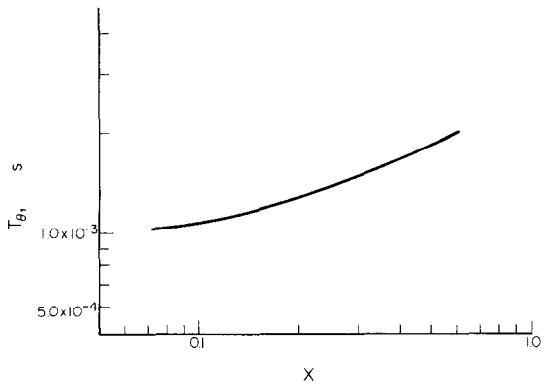

FIG. 15. Time scale, T_θ, of fluctuations vs downstream distance.

Figure 14 shows a measurement of the spectrum of temperature variance. Spectral measurements were made at $x = 0.049$, 0.098 and 0.197 for $r = 0.625$, 0.5 and 0.75. These spectra were normalised so that as $\omega T_\theta \to 0$, $\phi(\omega T_\theta) \to 1/\pi$. T_θ was determined from the $\omega \to 0$ asymptote of the unnormalised spectrum. This scaling collapsed the spectra on to the single curve shown in Fig. 14.

One may compare the temperature spectrum with the radial velocity spectrum (Fig. 4). They appear to be different in form. This is to be expected since the connection between velocity and temperature downstream of a line source is quite non-linear. The fact that the temperature spectrum is flatter than the velocity spectrum indicates that the randomly convected temperature plume produces temperature fluctuations which are "noisier" than the velocity fluctuations.

As a crude model, the trace of temperature versus time recorded by a measurement probe can be regarded as a sequence of random spikes (see Fig. 11 of [10]). The sharper the spikes, the flatter the spectrum of fluctuations. The average width of the spikes, is $2T_\theta$. As it is convected downstream, the instantaneous thermal plume will widen. Hence, on the basis of the above model, T_θ will increase. Our measurements of T_θ showed a large amount of scatter and are not quanti-

tatively reliable. However, measured values of T_θ consistently increased with x. An average profile of T_θ (averaged over measurements made near the centre of the mean thermal plume) is presented in Fig. 15.

Discussion of $\overline{T'^2}$ measurements

Fluctuation measurements have been presented at locations near to the source. Because all measured profiles appear symmetric in the r-direction, we assume they are not significantly affected by turbulence inhomogeneity. At stations further downstream inhomogeneity begins to play a role; but, temperature fluctuations have decayed drastically by the time these are reached.

Because of this near homogeneity, it is interesting to compare our measurements with those made by Uberoi and Corrsin [10] in decaying grid turbulence. Uberoi and Corrsin also used a line source. They found a nearly self-similar form for $\overline{T'^2}(y/\sigma)/\bar{T}^2(y=0)$ (see also [11]). This form had the appearance of a beheaded Gaussian, but no double peaks were found. On the plume axis, $y = 0$, $\overline{T'^2}/\bar{T}^2$ was approximately 0.4 at all distances downstream. This value is higher than any we observed. But Uberoi and Corrsin's grid ($M = 2.54$ cm) would have produced larger scale turbulence than our pipe, and this would tend to increase the ratio of fluctuation to mean. Thus, our data seem consistent with theirs.

5. CONCLUSIONS

Mean temperatures

It was found that mean dispersion from the wall source is described well by an eddy diffusion equation with parabolic diffusivity.

Dispersion from the elevated source is described by the Lagrangian theory of [5] and its extension to inhomogeneous turbulence by [7]. Near the source mean profiles appear Gaussian. Further from the source the peak temperature descends towards the wall and eventually the profile becomes uniformly mixed.

Temperature variance

Variance decays rapidly in the downstream direction.

The ratio of fluctuation to mean is greater for elevated than for wall sources.

The elevated source produces a double peaked, self similar profile of $\overline{T'^2}$.

The connection of centre-of-mass and relative dispersion with concentration fluctuations was discussed and used to describe the measurements of $\overline{T'^2}$. Large-scale eddies cause centre-of-mass dispersion and are responsible for producing temperature fluctuations. Small-scale eddies cause relative dispersion and are responsible for dissipation of fluctuations. They are also responsible for the double peak.

Acknowledgement—This work was supported by the United Kingdom Atomic Energy Authority.

REFERENCES

1. J. Laufer, The structure of turbulence in fully developed pipe flow, NACA tech. report 1174 (1954).
2. J. Sabot and G. Comte-Bellot, Intermittancy of coherent structures in the core region of fully developed turbulent pipe flow, *J. Fluid Mech.* **74,** 767 (1976).
3. H. B. Fischer, Longitudsnal dispersion and turbulent mixing in open-channel flow, *Ann. Rev. Fluid Mech.* **5,** 59 (1973).
4. A. G. Robbins and J. E. Fackerell, in *Mathematical Modelling of Turbulent Diffusion in the Environment*, pp. 55–114. Academic Press, New York (1979).
5. G. I. Taylor, Diffusion by continuous movements, *Proc. London Math. Soc.* **20,** 196 (1921).
6. D. J. Shlien and S. Corrsin, Dispersion measurements in a turbulent boundary layer, *Int. J. Heat Mass Transfer* **19,** 285 (1976).
7. P. A. Durbin and J. C. R. Hunt, Dispersion from elevated sources in neutral boundary layers, *J. Mech.* **19,** 679 (1980).
8. B. E. Launder, Topics in Applied Physics, in *Turbulence*, Vol. 12, chapter 6. Springer, Berlin (1976).
9. P. A. Durbin, A stochastic model of two-particle dispersion and concentration fluctuations in homogeneous turbulence, *J. Fluid Mech.* **100,** 279 (1980).
10. M. S. Uberoi and S. Corrsin, Diffusion from a line source in isotropic turbulence, NACA rept. 1142 (1953).
11. P. A. Libby, Diffusion in homogeneous turbulence, *Acta Astron.* **2,** 867 (1975).

DISPERSION EN AVAL DES SOURCES LINEAIRES DANS UN ECOULEMENT TURBULENT DE CONDUITE

Résumé—On présente des données sur la température moyenne et sur la variance en aval des sources linéaires dans un écoulement turbulent en conduite. On considère à la fois une paroi et une source élevée. La théorie connue de la dispersion est utilisée pour décrire les mesures de température moyenne: les mesures pour la source en paroi s'accorde bien avec le calcul d'une diffusion turbulente; les résultats obtenus avec la source élevée s'accordent avec les théories de [5] et [7]. On discute la relation entre le centre de masse et la variance de température. Les idées issues de cette discussion sont utilisées pour décrire qualitativement les mesures effectuées.

DISPERSION VON LINIENQUELLEN BEI DER TURBULENTEN ROHRSTRÖMUNG

Zusammenfassung—Es werden Daten über den Mittelwert und die Streuung des Temperaturfeldes stromabwärts von Linienquellen bei turbulenter Rohrströmung mitgeteilt. Betrachtet werden sowohl Quellen an der Wand als auch erhöhte Quellen. Die bestehende Dispersionstheorie wird benutzt, um unsere Messungen der Mitteltemperatur zu beschreiben. Messungen bei Wandquellen stimmen gut mit Scheindiffusionsberechnungen überein; Daten, die man von einer erhöten Quelle erhält, stimmen mit den Theorien von [5] und [7] überein. Der Zusammenhang zwischen Massenzentrum und relativer Dispersion in Abhängigkeit von der Temperaturstreuung wird erötert. Die Ideen, die aus dieser Erörterung hervorgehen, werden benutzt, um die gemessenen Daten qualitativ zu beschreiben.

ТУРБУЛЕНТНАЯ ДИФФУЗИЯ ТЕПЛА ОТ ЛИНЕЙНЫХ ИСТОЧНИКОВ ПРИ ТУРБУЛЕНТНОМ ТЕЧЕНИИ В ТРУБЕ

Аннотация — Представлены данные по средним и среднеквадратичным значениям температурного поля вниз по потоку за линейными источниками тепла при турбулентном течении в трубе. Рассматриваются два случая: источник на стенке и на некотором расстоянии от нее. Для объяснения полученных результатов измерений средних значений температуры используется известная полуэмпирическая теория турбулентного переноса, основанная на описании дисперсии пульсаций температуры. При этом показано, что результаты измерений для источника на стенке удовлетворительно описываются моделью вихревой вязкости. Экспериментальные данные, полученные для источника в потоке, находятся в соответствии с дисперсионными моделями [5] и [7]. Выводы, полученные из аналитического рассмотрения, используются для качественного объяснения экспериментальных результатов.